JGR Atmospheres

RESEARCH ARTICLE
10.1029/2024JD041305

Ice Crystal Habit Effects on the Resilience of Arctic Mixed-Phase Stratus Clouds in a One-Dimensional Model

Abhisek Das[1], **Eugene E. Clothiaux**[1], **and Jerry Y. Harrington**[1]

[1]Department of Meteorology and Atmospheric Science, The Pennsylvania State University, University Park, PA, USA

Key Points:

- Ice crystal habits affect dissipation, or glaciation, times of liquid water clouds in one-dimensional model runs of Arctic mixed-phase clouds
- Bulk adaptive model ice crystal habits and concentrations, as well as cloud-average temperatures, all play a role in liquid water path changes
- Subsidence velocity strengths also modulate Arctic mixed-phase cloud lifetimes

Supporting Information:

Supporting Information may be found in the online version of this article.

Correspondence to:

A. Das,
apd5662@psu.edu

Citation:

Das, A., Clothiaux, E. E., & Harrington, J. Y. (2025). Ice crystal habit effects on the resilience of Arctic mixed-phase stratus clouds in a one-dimensional model. *Journal of Geophysical Research: Atmospheres*, *130*, e2024JD041305. https://doi.org/10.1029/2024JD041305

Received 5 APR 2024
Accepted 23 FEB 2025

Author Contributions:

Conceptualization: Abhisek Das, Jerry Y. Harrington
Data curation: Abhisek Das, Jerry Y. Harrington
Formal analysis: Abhisek Das, Eugene E. Clothiaux, Jerry Y. Harrington
Funding acquisition: Eugene E. Clothiaux, Jerry Y. Harrington
Investigation: Abhisek Das, Eugene E. Clothiaux, Jerry Y. Harrington
Methodology: Abhisek Das, Eugene E. Clothiaux, Jerry Y. Harrington
Project administration: Eugene E. Clothiaux, Jerry Y. Harrington
Resources: Eugene E. Clothiaux, Jerry Y. Harrington
Software: Abhisek Das, Jerry Y. Harrington

Abstract Arctic single-layer mixed-phase clouds were studied using a one-dimensional model that incorporated the adaptive habit growth model for ice microphysics. The base case was from the Indirect and Semidirect Aerosol Campaign, and it was perturbed over a range of cloud-average temperatures, maximum (per model run) ice nuclei (IN) concentrations, and large-scale subsidence velocities. For each parameter combination, the model was iterated out to 48 hr, and the time, called the glaciation time, to complete disappearance of liquid recorded if this occurred within the 48 hr. Dependence of glaciation times on cloud-average temperatures from −30°C to −5°C, maximum IN concentrations from 0.10 to 30 L^{-1}, and strong–no subsidence, with both isometric and habit-dependent ice crystal growth, were investigated. For isometric crystal growth, the relationship between the critical maximum IN concentration (IN_{crit}), the maximum (per model run) IN concentration above which a mixed-phase cloud glaciated within a fixed model runtime, and cloud-average temperature was monotonic. IN_{crit} decreased with decreasing cloud-average temperature. Strengthening of subsidence led to a further decrease in IN_{crit} for every cloud-average temperature. For habit-dependent ice crystal growth, the relationship between IN_{crit} and cloud-average temperature was nonmonotonic. Ice crystals develop dendritic and columnar habits near −15°C and −7°C, respectively, and at these two temperatures, ice crystals grew and depleted supercooled liquid water faster than the case when ice crystals grew isometrically. This led to deep local minima in IN_{crit} around these two temperatures in the model runs. Habit-dependent ice crystal growth, coupled with changes in cloud-average temperature, IN_{crit}, and subsidence strength, led to significant changes in Arctic single-layer mixed-phase cloud lifetimes.

Plain Language Summary In this study, we investigated the glaciation of the Arctic single-layer mixed-phase clouds using a one-dimensional model incorporating the adaptive habit growth model for ice microphysics, which predicts the growth of ice crystals. We focused on the critical ice nuclei (IN) concentration for which the cloud glaciated completely due to the Wegener-Bergeron-Findeisen process. We also examined how changes in subsidence velocity with the effect of IN concentrations affected the Arctic mixed-phase cloud glaciation time. The glaciation time was found to be sensitive to the strengthening of subsidence velocity, maximum IN concentrations, and the cloud-average temperature. By varying the cloud-average temperature and IN concentrations across different subsidence strengths, we observed significant impacts on the critical IN concentration. Specifically, stronger subsidence and lower cloud-average temperature led to a reduction in the critical IN concentration, which resulted in faster cloud glaciation. Interestingly, the relationship between critical IN concentrations and cloud-average temperature varied when ice particles grew with patterns like dendrites or columns. Notably, at temperatures around −15°C and −7°C, the critical IN concentration values decreased drastically when the ice particles exhibited these specific habits.

1. Introduction

Arctic mixed-phase clouds strongly modulate the radiative environment of surface and boundary layers via their cloud radiative effect, that is, the difference in atmospheric irradiance between clear-sky and cloudy conditions (Intrieri et al., 2002; Shupe & Intrieri, 2004), with significant impacts on surface and boundary layer processes. The lifetimes of these clouds depend on the interactions among microphysics, radiation, and turbulence. These factors play an important role in Arctic mixed-phase cloud maintenance on timescales of hours (Curry & Herman, 1985; Morrison et al., 2012).

Because both liquid and ice particles coexist in Arctic mixed-phase clouds, they are colloidally unstable. Depositional growth of ice crystals after nucleation depletes liquid water content (LWC) through the Wegener-Bergeron-Findeisen (WBF) process. An increase in the concentration of ice nuclei (IN) depletes LWC faster, with

Supervision: Eugene E. Clothiaux, Jerry Y. Harrington
Validation: Abhisek Das, Eugene E. Clothiaux, Jerry Y. Harrington
Visualization: Abhisek Das, Eugene E. Clothiaux, Jerry Y. Harrington
Writing – original draft: Abhisek Das
Writing – review & editing: Abhisek Das, Eugene E. Clothiaux, Jerry Y. Harrington

a temperature dependence on the depletion rate (Korolev & Isaac, 2003; Sulia & Harrington, 2011). Previous studies have shown that reductions in LWC as a result of increasing IN concentrations weaken the circulation in the cloud layer due to weaker radiative cooling from the cloud top (Harrington & Olsson, 2001; Sulia et al., 2014). Weaker circulations, in turn, reduce the buoyant production of turbulent kinetic energy (TKE).

Turbulence in the cloud layer promotes entrainment, which increases cloud-top height (Stevens et al., 2005). The entrainment velocity is convolved with the large-scale subsidence velocity in the temporal evolution of Arctic mixed-phase clouds. Therefore, large-scale subsidence is also an important determinant in Arctic cloud lifetimes. The subsidence velocity provides a strong control on the height of the boundary layer. A weaker subsidence velocity typically leads to deepening of the boundary layer and larger LWCs in stratocumulus clouds (Bretherton et al., 2013). van der Dussen et al. (2016) show the impact of subsidence strength on the transition of stratocumulus to shallow cumulus clouds in the subtropical part of the Hadley cell. Despite the large-scale subsidence velocity being weaker over the Arctic than elsewhere, studies by Young et al. (2018) and Neggers et al. (2019) demonstrate its importance to Arctic mixed-phase clouds. In their large eddy simulation (LES), Young et al. (2018) found that increases in subsidence strength enhanced LWCs in these clouds, as stronger inversions resulting from stronger subsidence weakened the mixing of drier, warmer air into the cloud through entrainment. Yet, in another LES, Dimitrelos et al. (2020) showed that increases in subsidence decreased cloud lifetimes considerably. Details of both the physics and the environmental conditions in an LES are important determinants of simulation results.

Interactions between the processes heretofore mentioned are sensitive to cloud LWCs, which, in turn, are sensitive to the underlying microphysics. Accelerated depositional growth of primary planar habits around −15°C and columnar habits around −7°C (Bailey & Hallett, 2009) cause additional depletion of LWC compared to isometric ice crystal growth. Modeling ice crystals as spheres or using mass-size relations (Avramov & Harrington, 2010) precludes capturing the temperature-dependent growth of primary habits (Sulia & Harrington, 2011). Silber et al. (2021) demonstrate that around these temperatures (i.e., −15°C and −7°C) cloud LWCs decrease most rapidly as a result of larger depositional growth rates than those at surrounding temperatures. This habit-dependent growth is one explanation for the prominent low points in the observed frequency distribution of liquid-containing clouds (Silber et al., 2021). These observations and modeling results suggest that the combination of habit-dependent growth, cloud-average temperature, ice crystal concentration, and subsidence velocity has a strong impact on the longevity of supercooled liquid water in Arctic mixed-phase clouds. Most prior studies of habit-dependent influences on mixed-phase cloud maintenance focused on individual case studies (e.g., Avramov & Harrington, 2010; Sulia et al., 2014). To our knowledge, no studies have explored the influence of habit-dependent growth on mixed-phase clouds across a broad range of cloud-average temperatures, ice crystal concentrations, and subsidence velocities, which is the focus of our study.

Many models use diagnostic ice nucleation schemes based on temperature or supersaturation-dependent functions (Meyers et al., 1992). However, diagnostic ice nucleation schemes have shortcomings in modeling persistent ice formation in Arctic mixed-phase clouds (Fridlind et al., 2007). Studies also suggest that deposition ice nucleation acts too aggressively, producing copious ice crystals that easily desiccate the liquid cloud layer (Harrington et al., 1999). Simulations of single-layer mixed-phase clouds from the Mixed-Phase Arctic Cloud Experiment (Verlinde et al., 2007) showed that smaller increases in concentrations of deposition ice nuclei (IN) lead to dissipation of mixed-phase cloud layers (Prenni et al., 2007). Evidence now suggests that ice likely forms through immersion freezing in Arctic mixed-phase clouds, at least at temperatures below −10°C (de Boer et al., 2010; Murray et al., 2012). In de Boer et al. (2010), persistent ice nucleation in mixed-phase clouds was represented through a prognostic ice nucleation scheme, though this scheme consumed IN without replenishing them to observed levels in the cloud layer.

To better understand the effect of ice particle-driven dissipation of cloud LWC and persistent IN formation in the cloud layer, McFarquhar et al. (2011) and Ovchinnikov et al. (2014) used a diagnostic ice nucleation scheme to match observed ice particle concentrations in the Indirect and Semidirect Aerosol Campaign (ISDAC). These studies show that liquid clouds were stable for lower IN concentrations, and the liquid clouds glaciated when IN concentration increased, consistent with earlier studies (e.g., Pinto, 1998). Given the challenges and uncertainties in modeling heterogeneous ice formation (Cantrell & Heymsfield, 2005; Tan & Barahona, 2022; Zhang et al., 2020), we use the simplified parameterization from Ovchinnikov et al. (2014). This allows us to assess the importance of ice concentration influences combined with habit-dependent growth on mixed-phase cloud

longevity without the complicating feedback that may occur with more complex ice nucleation schemes. To assess these sensitivities, we perform model runs over a range of maximum (permitted per model run) IN concentrations.

LES models are able to well represent turbulence-microphysics interactions in Arctic mixed-phase clouds (e.g., Hoffmann, 2020; Rauterkus & Ansorge, 2020; Sulia et al., 2014), but they are computationally expensive. As a result, they are not optimal for exhaustive sensitivity studies. One-dimensional (single-column) models are of value in exploratory ensembles to develop hypotheses on the interactions among radiation, microphysics, and buoyancy in mixed-phase cloud systems. Previous studies have shown that, in comparison to LES models, one-dimensional models are able to simulate reasonably stratocumulus boundary layer clouds generated by turbulence in a mixed layer (Bechtold et al., 1996; Moeng et al., 1996). Bretherton et al. (1999) showed that one- and two-dimensional models simulated the evolution of the marine boundary layer inversion height accurately, and some one-dimensional models were able to predict deepening and decoupling of the boundary layer with an overestimated LWP. A more recent study by Neggers et al. (2017) showed that one-dimensional models are, in comparison to LES, able to capture the stratocumulus to shallow cumulus transition, though with some deficiencies. The main objective in our study is to identify cloud glaciation timescales based on changes in the nature of the ice crystal growth, maximum IN concentrations, cloud-average temperatures, and subsidence rates. The results motivate investigation of specific parameter sets using LESs.

Simpfendoerfer et al. (2019) investigated feedback among radiation, depositional heating, entrainment, and subsidence in Arctic mixed-phase clouds using the one-dimensional turbulence closure model of Golaz (1997) with the adaptive habit microphysics of Jensen et al. (2017). This study demonstrated that the one-dimensional model coupled to habit-evolving microphysics is able to produce the observed pattern of clear and cloudy states reported by Stramler et al. (2011) and Engström et al. (2014). Silber et al. (2021) used this model to show that the observed minima in liquid-containing single-layer Arctic clouds at −15°C and −7°C may be due to habit-dependent growth.

In our approach of exploring the ramifications of habit-dependent growth under different conditions on Arctic mixed-phase cloud longevity, we neglect the effects of large-scale moisture and energy transport and convergence on Arctic mixed-phase cloud lifetimes. Arctic mixed-phase cloud lifetimes are influenced by energy and moisture intrusions into the Arctic system. These intrusions cause increased air temperatures and cloudiness, which, in turn, lead to increased sea-ice melt and surface fluxes via increased downwelling radiation from the atmosphere to the surface (Henderson et al., 2021; Persson et al., 2017; Shupe et al., 2013). These changes at the surface do impact the properties of the clouds above them. Our focus is on the local microphysics, radiation, ice nucleation, and subsidence processes that would play out within Arctic single-layer mixed-phase clouds in tandem with the large-scale regime.

The 26 April 2008 ISDAC case study profile was associated with a single-layer mixed-phase cloud under strong subsidence, and previous LES studies based on it (e.g., Ovchinnikov et al., 2011; Sulia et al., 2014) did not consider the impact of lower subsidence rates, with their associated impacts on boundary layer growth and mixed-phase cloud longevity. Most importantly, prior studies have either investigated cloud glaciation, that is, complete dissipation or disappearance of liquid in a mixed-phase cloud, at specific cloud temperatures, or analyzed mixed-phase cloud lifetimes utilizing ensembles with simplified microphysics. Silber et al. (2021) did not address specifically how IN concentrations and habit-dependent growth produce stable (i.e., long-lasting) or unstable (i.e., glaciating) clouds. Therefore, the focus of this study is investigation of the impact of habit-dependent growth of ice crystals on cloud lifetimes over a wide range of cloud-average temperatures (−30°C to −5°C), maximum IN concentrations, and subsidence strengths.

The rest of the paper is organized as follows. The ISDAC case study description is given in Section 2, and Section 3 provides the salient features of the one-dimensional model along with its microphysical model details. In Section 4, we discuss how cloud-average temperature, IN concentration, and subsidence influence mixed-phase cloud glaciation times, that is, the time at which liquid in a mixed-phase cloud reaches 0 g m^{-2}, for both isometric and habit-dependent ice crystal growth. Our discussion and conclusions are in Section 5. Supporting Information S1 provides details on the one-dimensional model equations in Section SI1, along with additional analyses in Sections SI2 and SI3, and we refer readers to this information at appropriate points in the main article.

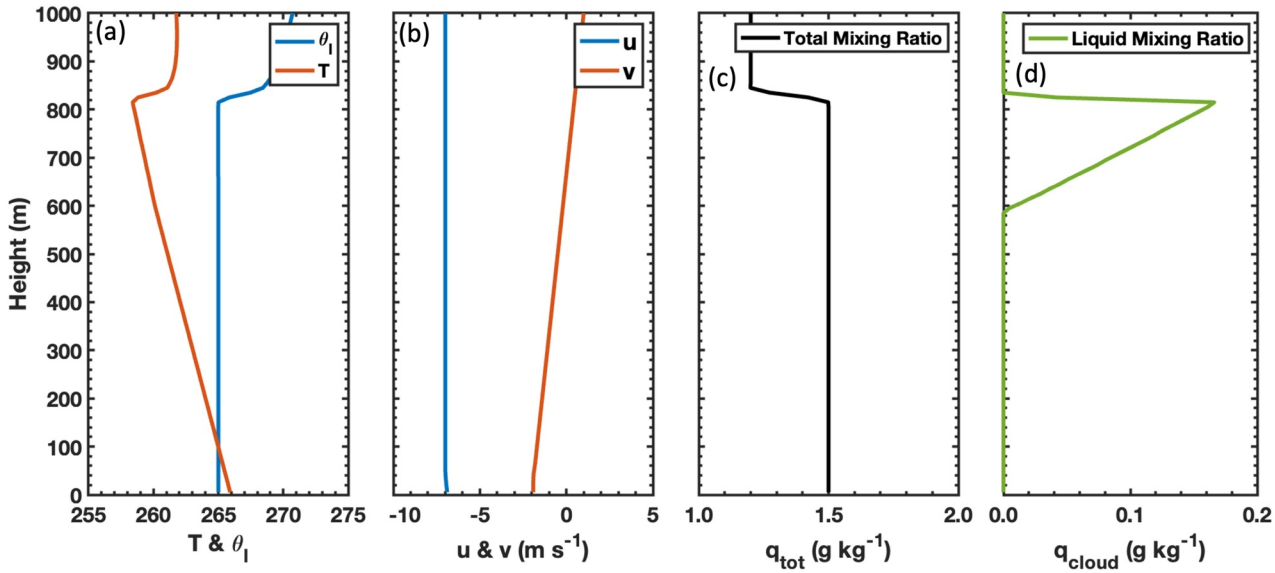

Figure 1. Profiles of (a) absolute (T) and liquid potential (θ_l) temperatures, (b) u- and v-wind components, (c) total water mixing ratio (q_{tot}), which includes water vapor, cloud liquid, and cloud ice, and (d) liquid (cloud) mixing ratio q_{cloud} of an idealized Indirect and Semidirect Aerosol Campaign sounding based on Ovchinnikov et al. (2014).

2. ISDAC Initialization and Construction of Clouds With Different Average Temperatures

The one-dimensional model (see Section 3 and Section SI1 in Supporting Information S1) is initialized with sounding data developed by Ovchinnikov et al. (2014, their Figure 1 and Appendix A1) for the 26 April 2008 ISDAC case. Given the exploratory nature of our study, we removed the slightly stable layer from 0 to 400 m of altitude (Figure 1). This eventually leads to formation of a mixed-layer with constant θ_l, and the time for this to happen depends on the subgrid scheme (Bechtold et al., 1992). Making θ_l constant at the time of initialization is equivalent to starting the model at a later time when clouds have already formed.

Aircraft observations of cloud microphysics on 8 April 2008 indicate a mixed-phase cloud from 600 to 800 m with LWCs from ~0.05 to 0.10 g m^{-3} in the upper half of the cloud and IWCs increasing from small values at the cloud top to ~0.06 g m^{-3} near the cloud base (McFarquhar et al., 2011, columns 10 and 11 of their Figure 13). The cloud liquid droplet and ice crystal concentrations ranged from ~100 to 200 cm^{-3} and from ~0.0 to 1.0 L^{-1}, respectively. The surface sensible and latent heat fluxes were ~10 W m^{-2} or less over an ice-covered sea. Following arguments in Ovchinnikov et al. (2014, their Appendix A2), we set the surface fluxes to zero in all of our model runs.

Boundary layer stratocumulus generally resides in regions of large-scale sinking motion (e.g., Schubert et al., 1979), and in one-dimensional and LES models, this motion is specified through large-scale divergence. The divergence is usually calculated from reanalysis output or other large-scale model analysis fields, implying potentially large uncertainties in this field in comparison to the observed cloud environment. Because our study explores the sensitivity of mixed-phase resilience to microphysics and forcing, we use a range of constant large-scale divergence values.

We define the *base case* as having no large-scale divergence (i.e., the divergence is set to 0.0 s^{-1}), which means cloud depth is set primarily by the cloud-scale circulations and entrainment. We label this case *sNone* (Table 1). The two remaining divergence values are 1.16×10^{-6} s^{-1}, labeled *sLow*, and 5.0×10^{-6} s^{-1}, the value used in Ovchinnikov et al. (2014) and Sulia et al. (2014) to represent ISDAC and labeled here as *sHigh*. The corresponding large-scale subsidence velocities at the inversion height of 850 m are approximately 1.0 and 4.1 mm s^{-1} (Table 1), consistent with the ranges presented in Fridlind et al. (2012, their Figure A4) and used in Simpfendoerfer et al. (2019). These three scenarios allow testing of the resilience of mixed-phase clouds to the degree of subsidence warming and drying of the cloud layer.

Table 1
Large-Scale Divergence Values Together With Their Associated Subsidence Velocities

Case	Divergence (s^{-1})	Subsidence velocity (mm s^{-1})	Inversion height (m)
sNone	0.0	0.0	825
sLow	1.16×10^{-6}	1.0	825
sHigh	5.0×10^{-6}	4.1	825

For the ISDAC case, the mixed-phase cloud temperature was near −15°C just beneath the cloud top (Figure 1a), a region where observed ice crystals had dendritic structures (McFarquhar et al., 2011). Temperatures near −15°C favor the rapid growth of dendritic ice crystals, making this case an appropriate one for investigating the impact of ice concentrations and single-crystalline habit growth on mixed-phase cloud longevity. To explore the impact of IN concentrations and subsidence on different temperature-dependent habit growth regimes, we changed the liquid cloud-average temperature. This latter quantity is defined as the average temperature of the initial liquid cloud layer (i.e., where the relative humidity RH ≥ 100%). We constructed synthetic soundings from the ISDAC sounding by changing the liquid cloud-average temperatures from −5°C to −30°C while adjusting the liquid-water potential temperatures to keep the initial RH profile fixed. The cloud top and cloud base heights remained fixed at 825 and 595 m, respectively. An example of the adjustment of the base case profile from the initial cloud top temperature near −15°C to a cloud-average temperature of −7°C is illustrated in Figure 2. We constructed synthetic soundings in 1°-C increments from −5°C to −30°C using this method. Each case, therefore, should have a similar cloud depth, but different crystalline habits will evolve based on the temperature. Observed IN concentrations ranged from much less than 1 L^{-1} to more than 10 L^{-1} (McFarquhar et al., 2011). Sulia et al. (2014) demonstrated that an IN concentration of 4 L^{-1} was sufficient to glaciate the mixed-phase cloud in their study when using the bulk adaptive habit model used here.

For our study, we chose maximum IN concentrations to range from 0.10 to 30 L^{-1}. The high maximum IN concentration of 30 L^{-1} is reasonable to study glaciation timescales at low cloud temperatures for both isometric and habit-dependent ice crystal growth (Harrington et al., 1999; Korolev & Isaac, 2003; Sulia & Harrington, 2011).

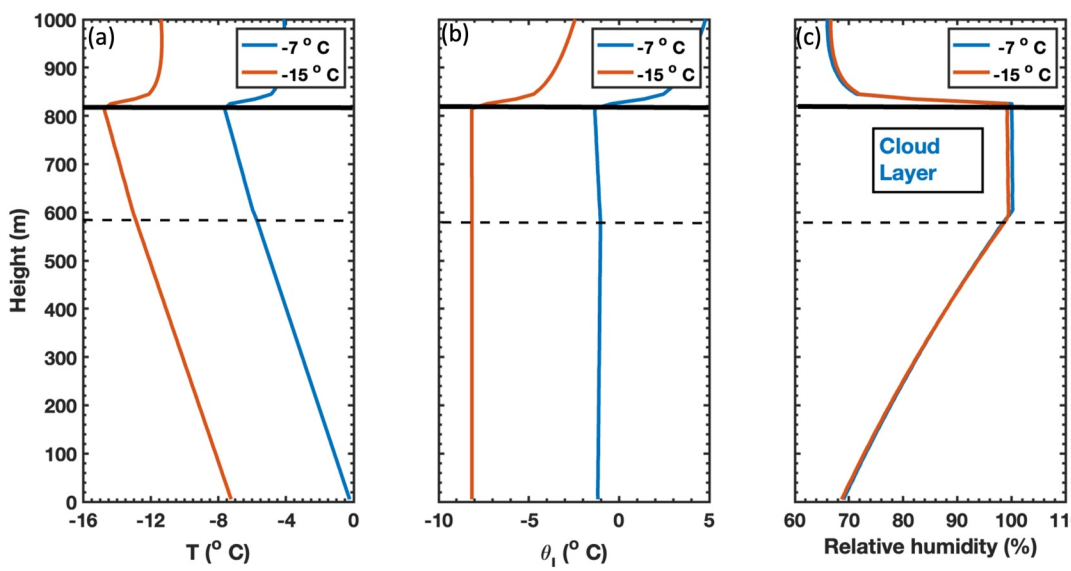

Figure 2. Different profiles of (a) temperature (T), (b) liquid potential temperature (θ_l), and (c) relative humidity with respect to liquid generated by keeping the relative humidity constant and setting the liquid cloud-average temperature to −7°C (i.e., column growth) and −15°C (i.e., planar growth, as observed).

3. The One-Dimensional Model and Microphysics

This study uses the one-dimensional turbulence closure model of Golaz (1997) with updates introduced by Simpfendoerfer et al. (2019). The model prognoses vertical profiles of ice-liquid potential temperature (θ_{il}), the total water mixing ratio (q_{tot}), and the u- and v-velocity components. This model depends upon a single-spatial coordinate; hence, it is called one-dimensional. For the ISDAC case study, drizzle, rain, snow, aggregate, graupel, and hail processes were unimportant. As a result, vertical profiles of the prognosed variables are used to diagnose a vertical profile of liquid cloud mixing ratios (q_{cloud}). This is a "condensation condensed" scheme where all of the water above liquid equilibrium is condensed as cloud water. This simplification needs to be borne in mind when interpreting the results, though it may have only a small impact on our results: Harrington (1997) and Harrington et al. (1999) found that droplet nucleation and droplet concentration had little impact on the evolution of mixed-phase clouds at −5°C and −15°C. If $q_{cloud} \geq 0.005$ g kg^{-1} and ice supersaturation is greater than or equal to 5% at a time step, ice crystals are initiated, leading to an increase in ice cloud mixing ratios (q_{ice}). The ice crystals grow and sediment in time based on either isometric- or habit-dependent growth. Note that nonzero, and significant, diagnostic values for q_{cloud} appear on the first model time step of 1 minute, whereas q_{ice} grows from a starting value of 0 g kg^{-1}. Details regarding the prognostic equations are given in Supporting Information S1.

The turbulent part of the thermodynamics, mixing ratios, and momentum in the one-dimensional equations of motion is closed by 1.5 order closure theory. The eddy transfer coefficients for momentum, heat, and mixing ratio are derived from a TKE $\boldsymbol{l}$-type closure approach, where $\boldsymbol{l}$ is a mixing length scale (Bechtold et al., 1992). Also, entrainment is linked to TKE at the top of the boundary layer. The buoyancy flux from thermal and dynamical instability is closed with an *all or nothing* scheme, which incorporates the ice-liquid potential temperature (θ_{il}) because it is a conserved variable during parcel movement (Golaz, 1997, Supporting Information S1). The momentum, heat, and moisture fluxes are input as boundary conditions, and these fluxes are set to zero at the top of the model domain.

The one-dimensional model microphysics is a single-moment (mass mixing ratio) bulk scheme for the cloud droplet, rain, aggregate, and graupel categories and a multiple-moment (mass mixing ratio, number concentration, and volume) bulk scheme for pristine ice crystals. We do not model hail because it did not occur. In the model microphysics, the cloud droplet concentration is specified, whereas the other hydrometeor categories, except for pristine ice, have fixed mean diameters. The cloud droplet mass mixing ratio is a diagnostic, saturation adjustment scheme (Walko et al., 1995). Rain is created through autoconversion, aggregates are formed and grow through collection interactions among aggregates and pristine ice crystals, and graupel is formed through the collection of cloud droplets by ice particles. Though these processes are included, negligible amounts of collision-coalescence, aggregation, and riming occurred during this case study period (drizzle was absent in the ISDAC experiment); hence, using a single-moment scheme for these categories has little impact. The size spectra for all hydrometeor categories follow a generalized gamma distribution function with a specified shape parameter. The shape parameters for cloud drops and pristine ice crystals are 2 and 4, respectively (Jensen et al., 2017). The details of the liquid, aggregation, and riming parameterizations are described in Walko et al. (1995), whereas the adaptive habit model that is used to model pristine ice is described in Jensen et al. (2017).

The growth of pristine ice crystals follows the adaptive habit approach pioneered by Chen and Lamb (1994). This method evolves the aspect ratio of ice crystals using measured ratios of the deposition coefficients for the basal and prism facets of ice crystals, and a deposition density that accounts for secondary habits (hollowing and branching arms). The bulk microphysical version of this theory is used here (Harrington et al., 2013; Jensen et al., 2017). The primary habits of the ice crystals along with their densities and fall speeds are evolved in time by predicting the number, mass, and two volume moments of the size spectrum. The latter two volume moments allow the aspect ratio and bulk effective density of the crystals to evolve in time. The deposition coefficients for the basal (α_c) and prism (α_a) faces of an ice crystal are functions of temperature and supersaturation, and the different growth rates on the basal and prism faces cause the development of planar or columnar shapes. Newly nucleated ice crystals begin as spheres, and then, the ice crystals grow depending on the aspect ratio (c/a) and the deposition coefficient ratio (α_c/α_a). In this way, the evolution of ice crystals in terms of mass growth and shape is physically based. For the case of isometric ice crystals, the aspect ratio (c/a) stays fixed to one while growing through vapor deposition. Under isometric ice crystal growth, the initial density of the ice crystals is set to

920 kg m^{-3}. Then, depending on the aspect ratio (c/a) and the vapor deposition rate, the density of the ice crystals evolves.

Given the limited understanding of precise IN nucleation processes in Arctic mixed-phase clouds, and with our primary goal being to explore the sensitivity of the liquid phase in mixed-phase clouds to varying IN concentrations, we employed a simplified immersion freezing ice nucleation parameterization based on the work of Ovchinnikov et al. (2011, 2014). In this scheme, nucleation occurs once the liquid mixing ratio is greater than 0.005 g kg^{-1} and ice supersaturation is greater than or equal to 5%. Then, if the ice crystal concentration in a layer is less than a maximum IN concentration, the number of ice particles nucleated is such that the total number of ice crystals in the layer equals the maximum IN concentration. Otherwise, no new ice crystals are nucleated, and the ice crystal concentration remains unchanged. The maximum IN concentration for a model run is arbitrary and can be varied by the user, though for case studies, it is set based on observed ice concentrations. For this study, we vary the maximum IN concentration across model runs. While such a nucleation scheme is admittedly simplistic, it does allow us to understand the impact of maximum IN concentration on mixed-phase cloud longevity.

A two-stream radiation scheme coupled with the microphysics is used to compute the infrared radiative heating rates (Harrington, 1997; Harrington & Olsson, 2001). To compute the optical properties of the spherical liquid water drops, we used Lorenz-Mie theory. For the habit-dependent ice crystals, with their different shapes, we used a modified version of anomalous diffraction theory to compute their optical properties (Harrington, 1997; Harrington & Olsson, 2001). We neglect solar (shortwave) radiation given the time of year (Arctic spring), for which solar heating is weak.

The height of the vertical domain is 2,500 m, and the vertical grid spacing is 10 m. The model time step is 5 s for dynamical and scalar evolution, whereas the radiative time step is 10 s. The longer radiative time step is used because the cloud fields generally do not change greatly over 10 s, and hence, a longer time step is sufficient to capture the longwave radiative cooling rates. The total model runtime is 48 hr.

4. Results of One-Dimensional Model Runs With Mixed-Phase Clouds

Most cloud microphysical schemes approximate the growth of ice crystals using either isometric shapes (Morrison et al., 2009; Solomon et al., 2009) or mass-size relationships (e.g., Avramov & Harrington, 2010). To determine the influence of habit on cloud-phase stability, we perform model runs with both isometric and habit-dependent ice crystal growth. As stated earlier, the maximum (per model run) IN concentration above which the LWP goes to zero within a fixed model runtime is defined as the *critical maximum IN concentration* (IN_{crit}). IN_{crit} is dependent on multiple factors, including ice crystal habit, cloud-average temperature, and subsidence strength determined by large-scale divergence. For each synthetic sounding with a unique cloud-average temperature, the one-dimensional model is run over a range of maximum IN concentrations and the three subsidence rates given above.

In what follows, we first show the microphysical process rates for both isometric and habit-dependent ice crystal growth to illustrate contributing factors to differences in LWC depletion rates (Section 4.1). We then illustrate the impacts these microphysical process changes have on turbulence process rates (Section 4.2). The setup of our one-dimensional model runs at a cloud-average temperature of −15°C is similar to the LESs of Ovchinnikov et al. (2011) and Sulia et al. (2014). We compare our results to theirs to assess whether or not our one-dimensional model has fidelity to more complex LESs (Section 4.3). In the last three sections, we characterize the following: sensitivity of LWP temporal evolution to cloud-average temperature, maximum IN concentration, and subsidence strength (Section 4.4); dependence of IN_{crit} on cloud-average temperature and subsidence strength for model runtimes of 8, 24, and 48 hr (Section 4.5); and dependence of liquid cloud glaciation time on cloud-average temperature, maximum IN concentration for a model runtime of 48 hr, and subsidence strength.

4.1. Microphysical Process Rates for Isometric and Habit-Dependent Ice Crystal Growth

For illustrative purposes, we select a case with a maximum IN concentration of 1 L^{-1} and a cloud-average temperature of −15°C. At this temperature, ice crystals grow with a dendritic habit and at a much faster rate than isometric ice crystals with an aspect ratio of 1. The vapor deposition rate for habit-dependent ice crystal growth is almost an order of magnitude larger than for isometric ice crystal growth at a height of 600 m (Figure 3a). After 90 min, the mean a-axis length in the layer from 500 to 600 m for habit-dependent ice crystal growth is, again,

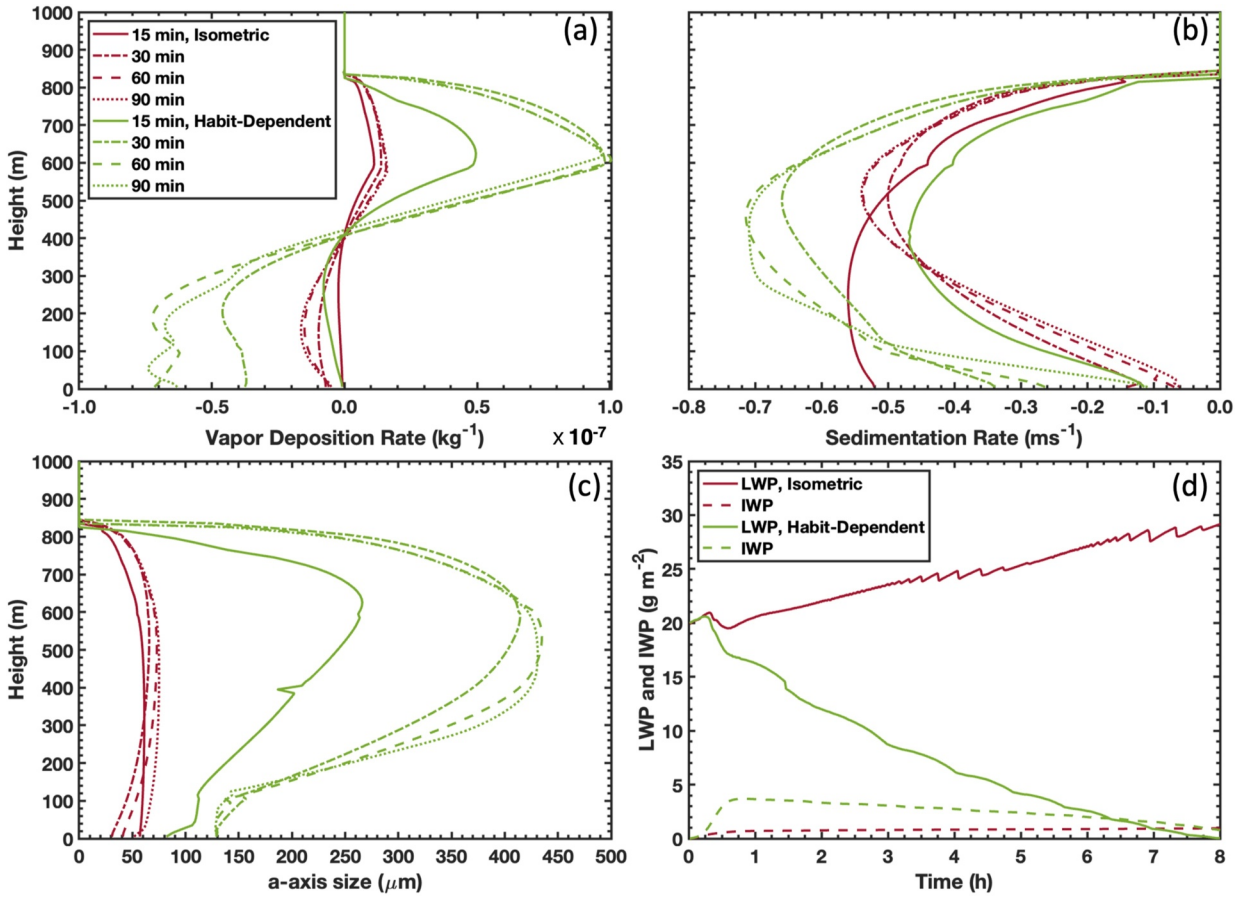

Figure 3. (a) Vapor deposition rate, (b) sedimentation rate, and (c) mean *a*-axis size for isometric (red) and habit-dependent (green) ice crystal growth 15, 30, 60, and 90 min into the model run for a maximum ice nuclei (IN) concentration of 1.0 L^{-1} and cloud-average temperature of −15°C. (d) Evolution of liquid water path and IWP for the same maximum IN concentration and cloud-average temperature.

much larger than for isometric ice crystal growth, approaching values around 450 μm as compared to 80 μm (Figure 3c). Early in the runs, the differences in mass-weighted sedimentation rates between the two particle types are smaller, though 90 min into them the habit-dependent ice crystals are falling faster at most altitudes. The isometric ice crystals are less massive than the habit-dependent ones, but they are also more compact, leading to sedimentation rates that are not so different between the two particle types. With similar residence times in the cloud layer, the habit-dependent ice crystals consume cloud liquid faster than the isometric ice crystals, thereby creating higher IWPs in time (Figure 3d). For this particular run, habit-dependent ice crystal growth is sufficiently rapid to glaciate the liquid cloud within 8 hr. The isometric and habit-dependent ice crystal growth rates explain the differences between the LWP and IWP for this case, as well as for different maximum IN concentrations and cloud-average temperatures.

4.2. Turbulence Process Rates for Isometric and Habit-Dependent Ice Crystal Growth

For the same maximum IN concentration of 1.0 L^{-1} and cloud-average temperature of −15°C as in Section 4.1, we characterize the evolution of the turbulent buoyancy fluxes and turbulent kinetic energies (TKEs) in the early stages of the model runs. As expected, the decrease in LWP for habit-dependent ice crystal growth versus time is much faster than for isometric ice crystal growth (Figure 3d). Figure 4 shows the turbulent buoyancy flux and TKE profiles at 15, 30, 60, and 90 min into the model runs. At 30 min into both model runs, the liquid water at the cloud top produces strong radiative cooling that promotes negative buoyancy fluxes at the cloud top. This downward-directed buoyancy can be enhanced by liquid evaporation due to cloud top entrainment of dry, warm air, and it can be offset by latent heating from depositional growth of ice. Indeed, the simulations of Harrington et al. (1999) suggest that net latent heating due to growing crystals can cause a decay in cloud-scale circulations.

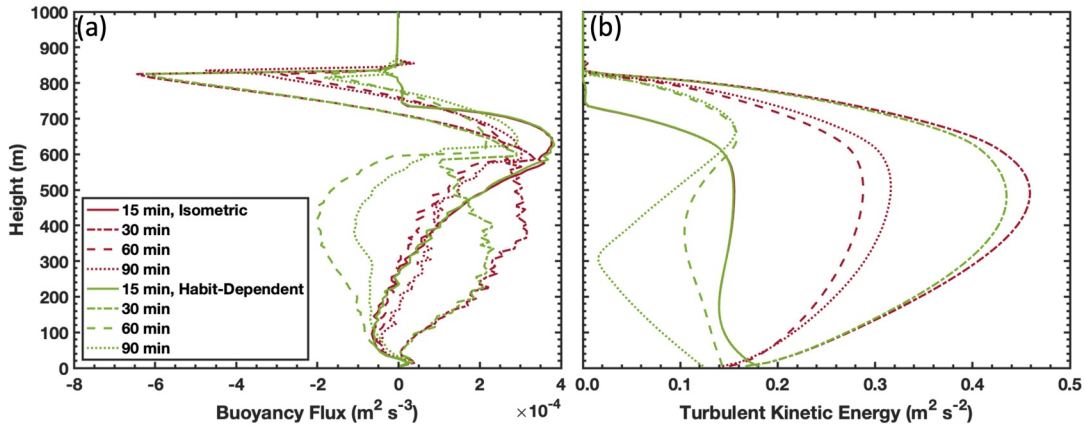

Figure 4. Turbulence process rates for isometric and habit-dependent ice crystal growth for an ice nuclei concentration of 1.0 L^{-1} and cloud-average temperature of −15°C. (a) Turbulent buoyancy fluxes and (b) turbulent kinetic energies 15, 30, 60, and 90 min into the model runs.

This is a steady feature in both runs throughout the first 90 min. In the subcloud layer, sublimation rates for the habit-dependent ice crystals are much larger than for isometric particles, leading to negative buoyancy fluxes and much lower TKEs for the habit-dependent ice crystal growth run. This weakening of subcloud layer dynamics leads to a loss of upward-directed moisture supply at the cloud base, and the loss of liquid from the high vapor deposition rates at the cloud base in the habit-dependent ice crystal run is not replaced. The liquid water contents in this case decrease from the cloud base upward.

4.3. LWP/IWP Sensitivity to Maximum IN Concentration at −15°C Cloud-Average Temperature

The results in Section 4.1 indicate that LWCs in mixed-phase clouds are lower for habit-dependent than isometric ice crystal growth because LWC depletion occurs more readily under habit-dependent ice crystal growth. These results are made explicit in Figures 5a and 5b, where we focus on the influence of maximum IN concentration at the two cloud-average temperatures that produce the greatest habit-dependent growth, namely −7°C and −15°C. To facilitate comparison of our LWP time series with those of the LESs by Ovchinnikov et al. (2011) and Sulia et al. (2014), we show LWP and IWP time series for 8 hr, maximum IN concentrations ranging up to 10 L^{-1}, and high (sHigh) subsidence, as these values encompass ones used in the two LESs.

Focusing on LWP and IWP evolution under isometric ice crystal growth for a cloud-average temperature of −15°C (Figures 5a and 5c, dashed lines), the liquid cloud glaciates in 4 hr for a maximum IN concentration of 10 L^{-1}. In Sulia et al. (2014, their Figure 3a), the liquid cloud does not glaciate within 8 hr for an IN concentration of 10 L^{-1}, though the LWP does decrease from 20 to 15 g m^{-2}. For all IN concentrations below 10 L^{-1}, the LWPs in both studies increase in time (cf., our Figure 5a with their Figure 3a). For these cases, the increase in cloud LWCs is a result of cloud top radiative cooling and cloud top entrainment.

Under isometric ice crystal growth, the IWPs in both studies are similar for similar IN concentrations, starting at 0 g m^{-2} and growing up to approximately 0.75–1.0 and 4.0–5.0 g m^{-2} for IN concentrations of 1 and 10 L^{-1}, respectively (cf., our Figure 5c with their Figure 3b). For isometric ice crystal growth at a cloud-average temperature of −7°C, glaciation does not occur in our study for any IN concentration, and LWPs increase and IWPs decrease relative to a cloud-average temperature of −15°C.

Relative to isometric ice crystal growth, habit-dependent ice crystal growth depletes liquid faster, thereby leading to lower LWPs (Figure 5b) and higher IWPs (Figure 5d). For a cloud-average temperature of −15°C, at which ice crystals grow with a dendritic habit, glaciation takes place in our study for all maximum IN concentrations, except for the lowest one of 0.50 L^{-1}. In Sulia et al. (2014), their IN concentrations of 4 and 10 L^{-1} lead to glaciation, whereas their IN concentration of 1 L^{-1} does not (their Figure 5a). Though Ovchinnikov et al. (2011) used a different growth model for ice crystal columns, plates, and dendrites in their LES simulations, their liquid cloud glaciates by ∼8 hr for an IN concentration of 2 L^{-1}, whereas for an IN concentration of 0.5 L^{-1}, there is almost no change in LWP throughout the 7 hr of LES simulation time (their Figure 5a). These results are not inconsistent

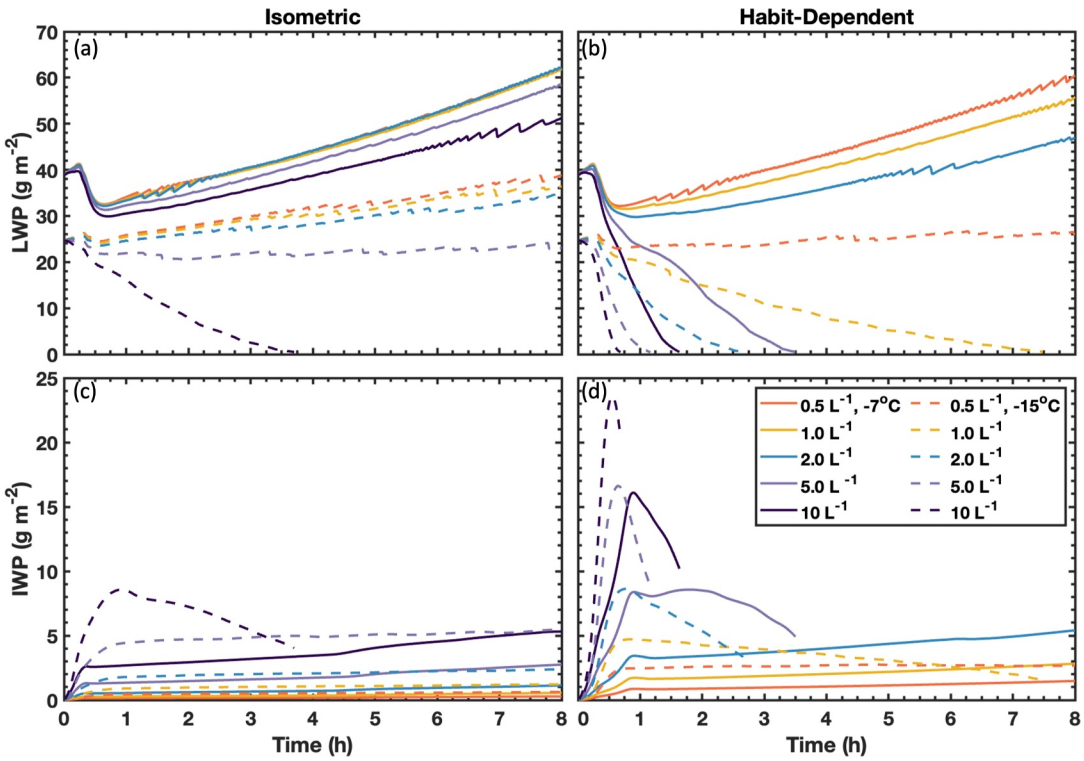

Figure 5. Temporal evolution of (a and b) liquid water path and (c and d) IWP for (left column) isometric and (right column) habit-dependent ice crystal growth at cloud-average temperatures of −7°C (solid lines) and −15°C (dashed lines) under sHigh subsidence for several maximum ice nuclei concentrations.

with those of Sulia et al. (2014) or our study. Similar to Ovchinnikov et al. (2011), the LWP for a maximum IN concentration of 0.5 L^{-1} also does not change much throughout the first 8 hr of our model run. Evolution of the LWP for our maximum IN concentration of 1 L^{-1} is similar to that for the IN concentration of 2 L^{-1} in Ovchinnikov et al. (2011). In summary, critical maximum IN concentrations for Sulia et al. (2014), Ovchinnikov et al. (2011), and our study fall in the range of ∼4.0, ∼2.0, and 0.5–1.0 L^{-1}, respectively, for a cloud-average temperature of −15°C and a model runtime of 8 hr.

Time evolution of the IWPs for habit-dependent growth in Sulia et al. (2014, their Figure 5b), Ovchinnikov et al. (2011, their Figure 5b), and our study (Figure 5d) at a cloud-average temperature of −15°C shows similar trends. In all three studies, IWPs start from 0 g m^{-2} and initially increase. At the maximum IN concentration for which the liquid cloud does not glaciate (1 L^{-1} in Sulia et al. (2014), 0.5 L^{-1} in Ovchinnikov et al. (2011), and 0.5 L^{-1} in our study), the IWPs increase monotonically in the beginning and plateau toward the end. For the maximum IN concentrations given above, Sulia et al. (2014), Ovchinnikov et al. (2011), and our study attain IWPs of approximately 5, 2.5, and 3 g m^{-2}, respectively, by the end 7–8th hr of model runtime. At the first (critical) maximum IN concentration for which the liquid clouds glaciate (4 L^{-1} in Sulia et al. (2014), 2 L^{-1} in Ovchinnikov et al. (2011), and 1 L^{-1} in our study), IWPs initially increase at a greater rate than for smaller maximum IN concentrations, reach a maximum value, and then decrease to the time of glaciation. The maximum (glaciation time) IWPs for the maximum IN concentrations above are approximately 12 (1), 8 (4), and 4 g m^{-2} (2 g m^{-2}) for Sulia et al. (2014), Ovchinnikov et al. (2011), and our study, respectively. In our study, a maximum IN concentration of 2 L^{-1} has values of approximately 9 g m^{-2} (3 g m^{-2}), whereas a maximum IN concentration of 5 L^{-1} has values of approximately 15 g m^{-2} (9 g m^{-2}).

Increasing the cloud-average temperature from −15°C to −7°C, a temperature at which ice crystals grow with a columnar habit, both increases the time to glaciation and increases the maximum IN concentration necessary to completely remove the liquid within 8 hr (Figure 5b, solid lines). For a cloud-average temperature of −7°C, the critical maximum IN concentration falls within the range 2.0–5.0 L^{-1}. Moreover, the glaciation times for

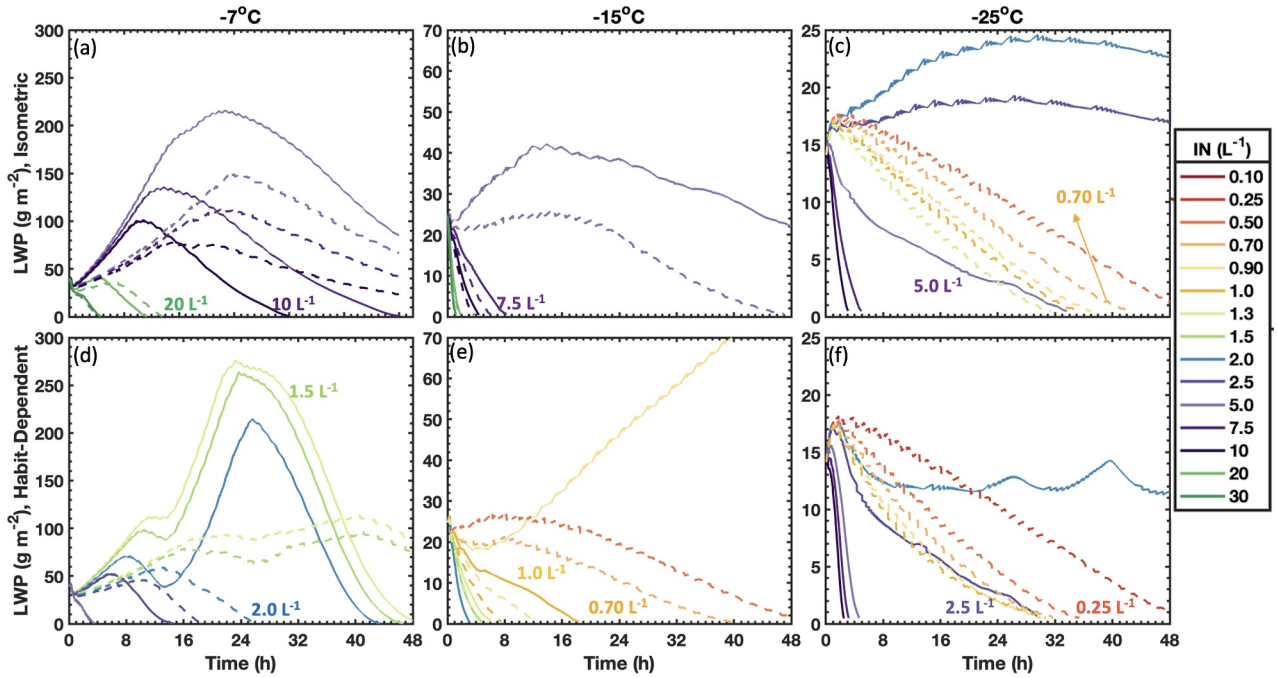

Figure 6. Liquid water path time series for (a–c) isometric and (d–f) habit-dependent ice crystal growth at cloud-average temperatures of (a and d) −7°C, (b and e) −15°C, and (c and f) −25°C for a range of ice nuclei concentrations from 0.1 to 30 L^{-1} and the two subsidence values, sLow (solid lines) and sHigh (dashed lines). Labels for the sLow and sHigh IN_{crit} values for the 48-hr runtimes are provided in each panel.

maximum IN concentrations of 5 and 10 L^{-1} at −7°C are more than double compared with a cloud-average temperature of −15°C (Figure 5b, cf., solid and dashed lines).

Under habit-dependent growth, maximum IN concentrations and cloud-average temperatures that do not lead to complete glaciation of the liquid clouds result in insufficient depositional growth. There are just too few ice crystals produced to do so. As cloud LWPs drop below 40 g m^{-2}, liquid clouds are no longer opaque across the infrared (Persson et al., 2002; Turner et al., 2007). As a result, cloud radiation emission rates decrease and radiation-induced circulations within the cloud weaken (similar to Harrington et al., 1999). This is an important reason why high maximum IN concentrations, which lead to lower LWPs, more readily lead to cloud glaciation and dissipation (Sulia et al., 2014).

4.4. LWP Sensitivity to Cloud-Average Temperatures and Subsidence

Evolution of the cloud LWPs over 48 hr of model runtime depends sensitively and nonlinearly on maximum IN concentration, cloud-average temperature, and subsidence strength (Figure 6). A general feature of all LWP time series is a rise to a global maximum followed by a fall toward 0 g m^{-2}, with LWP rates of change and the locations of the LWP global maximum moving to greater times with decreasing maximum IN concentrations. Focusing first on the cloud-average temperature of −7°C for the 48 hr model runs (Figures 6a and 6d), IN_{crit} values for isometric ice crystal growth are higher than those for habit-dependent growth. Changing ice particle growth from isometric to habit-dependent causes a decrease in IN_{crit} from 10 to 1.5 L^{-1} for sLow and 20 to 2.0 L^{-1} for sHigh. At this temperature, the maximum IN concentration necessary to glaciate the liquid cloud increases with increasing subsidence.

At a cloud-average temperature of −15°C (Figures 6b and 6e), IN_{crit} is 7.5 L^{-1} for both sLow and sHigh under isometric growth, with the time to glaciation slightly shorter for sHigh. Note that the maximum IN concentration of 5.0 L^{-1} nearly glaciates the liquid cloud within 48 hr under sHigh but not sLow. For habit-dependent growth at −15°C, the IN_{crit} values are 1.0 and 0.7 L^{-1} for sLow and sHigh, respectively. For a cloud-average temperature of −25°C (Figures 6c and 6f), the IN_{crit} values for isometric ice crystal growth are 5.0 and 0.7 L^{-1} for sLow and sHigh, respectively, whereas for habit-dependent growth they are 2.5 and 0.25 L^{-1}, respectively. These results illustrate the nonlinear dependence of IN_{crit} on cloud-average temperature, especially for habit-dependent ice

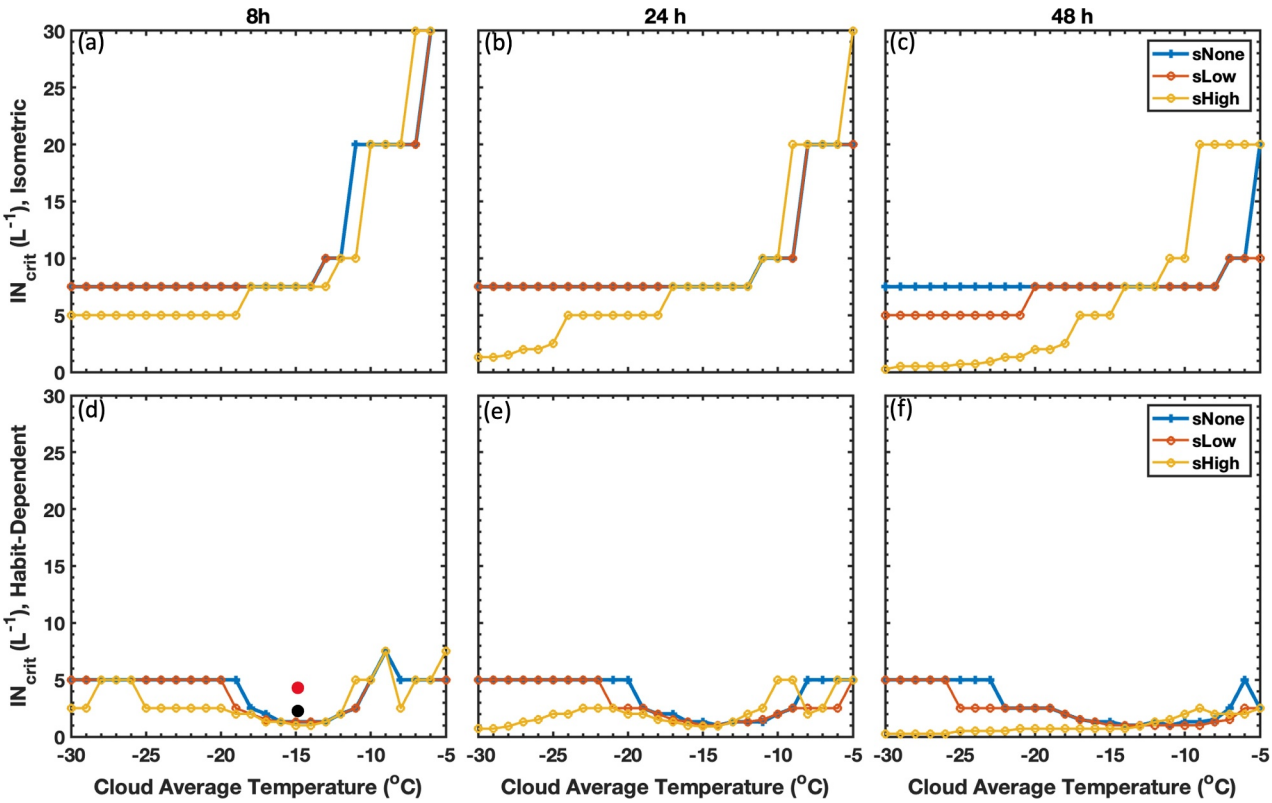

Figure 7. Relationship between IN_{crit} and cloud-average temperature for (a–c) isometric and (d–f) habit-dependent ice crystal growth for model runtimes of (a and d) 8 hr, (b and e) 24 hr, and (c and f) 48 hr for the three subsidence rates. The blue line indicates zero subsidence (sNone), the red line low subsidence (sLow), and the yellow line high subsidence (sHigh). The IN_{crit} values estimated from the works of Ovchinnikov et al. (2011) and Sulia et al. (2014) are represented by the black and red dots, respectively, in panel (d).

crystal growth for which the relationship is nonmonotonic. In the next section, we illustrate the sensitive dependence of IN_{crit} on model runtime, cloud-average temperature, and subsidence strength.

4.5. IN_{crit} Concentrations for Isometric and Habit-Dependent Ice Crystal Growth

Figure 7 presents a compact summary of all of the model run results illustrating the dependence of IN_{crit} on cloud-average temperature and subsidence strength. Recall that IN_{crit} is the maximum IN concentration for a model run above which a liquid cloud completely glaciates within the model runtime. As model runtimes increase, IN_{crit} either stays the same or decreases as liquid clouds with smaller maximum IN concentrations glaciate. As a result, $IN_{crit,8h} \geq IN_{crit,24h} \geq IN_{crit,48h}$ in Figure 7. For isometric ice crystal growth (Figures 7a–7c), IN_{crit} monotonically decreases with decreasing temperature for all model runtimes and subsidence strengths. For cloud-average temperatures in the range of −18°C and less, liquid clouds with maximum IN concentrations less than 7.5 L^{-1} are slow to glaciate under no (sNone) or low (sLow) subsidence. However, at these temperatures, liquid clouds are glaciating at ever lower values of IN_{crit} under strong (sHigh) subsidence with increasing model runtimes. Across the cloud-average temperature range from −5°C to −10°C, changes in IN_{crit} are different, with liquid clouds now slow to glaciate under high (sHigh) subsidence for maximum IN concentrations less than 20 L^{-1}. At this higher temperature range, IN_{crit} decreases with model runtime for sNone and sLow, with drops in IN_{crit} over 10 L^{-1} from 8 to 48 hr of runtime.

Relative to isometric ice crystal growth, habit-dependent ice crystal growth leads to a broad minimum in IN_{crit} over the cloud-average temperature range from −10°C to −20°C for all subsidence strengths, though the lowest two subsidence strengths lead to deeper minima (Figures 7d–7f). This feature is stable across all model runtimes. Another relatively stable feature across the three model runtimes is the two local maxima in IN_{crit} at −5°C and −10°C under high (sHigh) subsidence.

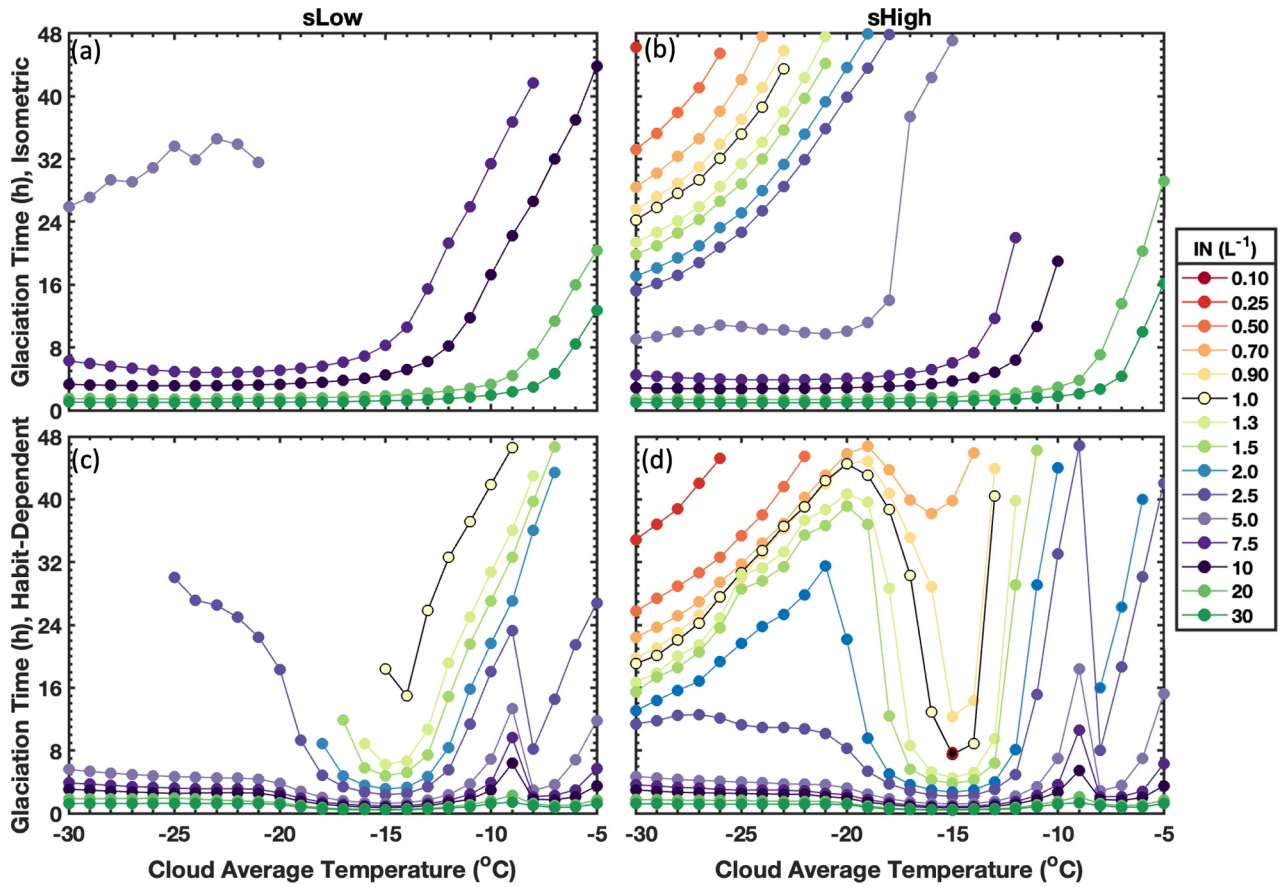

Figure 8. Glaciation time versus cloud-average temperature for (a and b) isometric and (c and d) habit-dependent ice crystal growth under (left column) low and (right column) high subsidence strengths over a range of maximum ice nuclei (IN) concentrations from 0.10 to 30 L^{-1}. The glaciation times estimated from the works of Ovchinnikov et al. (2011) and Sulia et al. (2014) are represented by the black and red dots, respectively, in panel (d). Both times are approximately equal to the glaciation time in our study for a maximum IN concentration of 1 L^{-1} at a cloud-average temperature of −15°C.

4.6. Glaciation Times for Isometric and Habit-Dependent Ice Crystal Growth

We now characterize liquid cloud glaciation times versus cloud-average temperatures from −5°C to −30°C for a range of maximum IN concentrations and model runtimes out to 48 hr.

For isometric ice crystal growth under low (sLow) subsidence (Figure 8a), mixed-phase clouds are maintained for all cloud-average temperatures as long as the maximum IN concentrations are below 5.0 L^{-1}. In the temperature range from −20°C to −30°C, glaciation times for a maximum IN concentration of 5.0 L^{-1} are around 30 hr. For higher maximum IN concentrations across this temperature range, glaciation times drop sharply to 6 hr and less. As cloud-average temperatures rise from −15°C to −5°C, it takes longer for a given maximum IN concentration to desiccate the liquid cloud. As a result, glaciation times increase monotonically with increasing temperatures across this range. Under high (sHigh) subsidence (Figure 8b), the biggest changes occur across the temperature range from −20°C to −30°C, as liquid clouds are now glaciating at ever smaller maximum IN concentrations with decreasing temperature across this range. Moreover, the glaciation time for a maximum IN concentration of 5.0 L^{-1} has dropped by 20 hr down to about 10 hr across this range. For the higher temperature range from −10°C to −5°C, maximum IN concentrations of 7.5 and 10 L^{-1} no longer desiccate the liquid cloud. Glaciation times for these maximum IN concentrations have now increased beyond 48 hr.

Habit-dependent ice crystal growth leads to shorter glaciation times at all maximum IN concentrations, all cloud-average temperatures, and all subsidence strengths in comparison to isometric ice crystal growth (cf., Figures 8a–8d). Features in Figures 7d–7f are reflected in features in Figures 8c and 8d. For maximum IN concentrations as low as 1.3 L^{-1}, glaciation times are shorter than ∼6 hr at temperatures near −15°C under both low (sLow) and high (sHigh) subsidence. With an increase in subsidence from sLow to sHigh, the glaciation time for a maximum

IN concentration of 1.0 L^{-1} drops from ~18 to ~8 hr at a cloud-average temperature of −15°C. At −15°C, a maximum IN concentration of 0.90 L^{-1} does not glaciate the liquid cloud within 48 hr under low subsidence, but does glaciate it in just over 10 hr under high subsidence. Local maxima in IN_{crit} values present in Figures 7d–7f at cloud-average temperatures of −5°C and −10°C have corresponding features in the glaciation times of Figures 8c and 8d. Fixed maximum IN concentrations of 2.0 L^{-1} and greater have local maxima in their glaciation times at these two temperatures, with the magnitude of the maxima decreasing with increasing maximum IN concentration.

5. Discussion and Conclusions

We performed one-dimensional model runs of Arctic single-layer mixed-phase stratiform clouds using the one-dimensional model of Golaz (1997) with updates from Simpfendoerfer et al. (2019). Our model atmosphere is based on the ISDAC 26 April 2008 case study period, and our model runtimes are out to 48 hr. During ISDAC, surface fluxes were negligible and radiative cooling at the cloud top was the main driver of circulations in the cloud and subcloud layers. Liquid cloud resilience was strongly dependent on isometric versus habit-dependent ice crystal growth (similar to Sulia and Harrington (2011) and Sulia et al. (2014)), as well as cloud-average temperature, maximum IN concentration, and large-scale subsidence. In particular, habit-dependent ice crystal growth desiccates liquid clouds rapidly and at lower maximum IN concentrations at cloud-average temperatures around −15°C and −7°C than for isometric ice crystal growth.

We based our one-dimensional model runs on similar atmospheric and microphysical properties to those in the LES simulations of Ovchinnikov et al. (2011) and Sulia et al. (2014), enabling a meaningful comparison of our results to theirs. For habit-dependent ice crystal growth, a maximum IN concentration of 2 L^{-1} in the Ovchinnikov et al. (2011) study and 4 L^{-1} in the Sulia et al. (2014) study desiccates the liquid cloud in ~8 hr. In our one-dimensional model runs, an IN concentration of 1.0 L^{-1} does so. Similar to Ovchinnikov et al. (2011), a maximum IN concentration of 0.5 L^{-1} in our study leads to little change in LWP. All three studies exhibit a faster rise in IWP to higher values followed by a faster fall with increasing maximum IN concentrations beyond the critical one. And similar to Sulia et al. (2014), we find that it takes significantly higher maximum IN concentrations at a cloud-average temperature of −15°C to desiccate liquid clouds under isometric ice crystal growth than habit-dependent growth. Overall, we find similar tendencies in LWP and IWP changes with changing maximum IN concentrations as those found in the LES simulations of Ovchinnikov et al. (2011) and Sulia et al. (2014). One consistent difference of our results in comparison to those of Sulia et al. (2014) is that our one-dimensional model runs require smaller maximum IN concentrations to desiccate the liquid clouds under both isometric and habit-dependent ice crystal growth.

Given the robust minima in liquid cloud glaciation times near −15°C and −7°C for fixed maximum IN concentration under both low (sLow) and high (sHigh) subsidence, we hypothesize similar minima will occur in comparable LES simulations. Based on our results, promising cloud-average temperatures to test the LES simulations are −5°C, −8°C, −10°C, −15°C, −20°C, and −30°C for maximum IN concentrations of 1, 2, and 4 L^{-1}. Because of the long glaciation times around −10°C and −20°C in our results, the LES simulations may need to be run out to 48 hr or longer. They would be expensive, but they would provide a test of whether or not the turbulence and entrainment parameterizations in the one-dimensional model using TKE 1.5 closure are able to reproduce results of a model that explicitly simulates the turbulent eddies.

Applying different LES models to the ISDAC case study period using bulk and bin microphysics schemes demonstrated how important the ice nucleation scheme and ice crystal size distribution are in the study of Arctic mixed-phase clouds (Ovchinnikov et al., 2014). Therefore, differences among LES models will lead to differences in their simulations. As such, there are uncertainties in their results, thereby introducing uncertainties into using them as a standard for comparison as we have done for this study.

Data Availability Statement

All simulation outputs for the single-column model are available through the Penn State Data Commons via the URL https://doi.org/10.26208/C000-D571 (Das et al., 2025).

Acknowledgments
The authors are grateful for the comments provided by the reviewers, which substantially improved the content of this manuscript. This research was supported by the National Science Foundation through Grants AGS-1824243 and AGS-2128347, the Department of Energy Atmospheric Systems Research through Grant DE-SC0023020, and by NASA through Grant 80NSSC19K0728.

References

Avramov, A., & Harrington, J. Y. (2010). Influence of parameterized ice habit on simulated mixed phase Arctic clouds. *Journal of Geophysical Research*, *115*(D3), D03205. https://doi.org/10.1029/2009jd012108

Bailey, M. P., & Hallett, J. (2009). A comprehensive habit diagram for atmospheric ice crystals: Confirmation from the laboratory, AIRS II, and other field studies. *Journal of the Atmospheric Sciences*, *66*(9), 2888–2899. https://doi.org/10.1175/2009jas2883.1

Bechtold, P., Krueger, S. K., Lewellen, W. S., Van Meijgaard, E., Moeng, C. H., Randall, D. A., et al. (1996). Modeling a stratocumulus topped PBL: Intercomparison among different one-dimensional codes and with large eddy simulation. *Bulletin of the American Meteorological Society*, *77*(9), 2033–2042. https://doi.org/10.1175/1520-0477-77.9.2033

Bechtold, P., Pinty, J. P., & Fravalo, C. (1992). A model of marine boundary-layer cloudiness for mesoscale applications. *Journal of the Atmospheric Sciences*, *49*(18), 1723–1744. https://doi.org/10.1175/1520-0469(1992)049<1723:amombl>2.0.co;2

Bretherton, C. S., Blossey, P. N., & Jones, C. R. (2013). Mechanisms of marine low cloud sensitivity to idealized climate perturbations: A single-LES exploration extending the CGILS cases. *Journal of Advances in Modeling Earth Systems*, *5*(2), 316–337. https://doi.org/10.1002/jame.20019

Bretherton, C. S., Krueger, S. K., Wyant, M. C., Bechtold, P., Van Meijgaard, E., Stevens, B., & Teixeira, J. (1999). A GCSS boundary-layer cloud model intercomparison study of the first ASTEX Lagrangian experiment. *Boundary-Layer Meteorology*, *93*(3), 341–380. https://doi.org/10.1023/a:1002005429969

Cantrell, W., & Heymsfield, A. (2005). Production of ice in tropospheric clouds: A review. *Bulletin of the American Meteorological Society*, *86*(6), 795–808. https://doi.org/10.1175/bams-86-6-795

Chen, J. P., & Lamb, D. (1994). The theoretical basis for the parameterization of ice crystal habits: Growth by vapor deposition. *Journal of the Atmospheric Sciences*, *51*(9), 1206–1222. https://doi.org/10.1175/1520-0469(1994)051<1206:ttbftp>2.0.co;2

Curry, J. A., & Herman, G. F. (1985). Relationships between large-scale heat and moisture budgets and the occurrence of Arctic stratus clouds. *Monthly Weather Review*, *113*(9), 1441–1457. https://doi.org/10.1175/1520-0493(1985)113<1441:rblsha>2.0.co;2

Das, A., Clothiaux, E. E., & Harrington, J. Y. (2025). Adaptive habit microphysics evolution in Arctic stratus within the single column model of Golaz (1997) [Dataset]. *Penn State Data Commons*. https://doi.org/10.26208/C000-D571

de Boer, G., Hashino, T., & Tripoli, G. J. (2010). Ice nucleation through immersion freezing in mixed-phase stratiform clouds: Theory and numerical simulations. *Atmospheric Research*, *96*(2–3), 315–324. https://doi.org/10.1016/j.atmosres.2009.09.012

Dimitrelos, A., Ekman, A. M., Caballero, R., & Savre, J. (2020). A sensitivity study of Arctic air-mass transformation using large Eddy simulation. *Journal of Geophysical Research: Atmospheres*, *125*(6), e2019JD031738. https://doi.org/10.1029/2019jd031738

Engström, A., Karlsson, J., & Svensson, G. (2014). The importance of representing mixed-phase clouds for simulating distinctive atmospheric states in the Arctic. *Journal of Climate*, *27*(1), 265–272. https://doi.org/10.1175/jcli-d-13-00271.1

Fridlind, A. M., Ackerman, A. S., McFarquhar, G., Zhang, G., Poellot, M. R., DeMott, P. J., et al. (2007). Ice properties of single-layer stratocumulus during the mixed-phase Arctic cloud experiment: 2. Model results. *Journal of Geophysical Research*, *112*(D24), D24202. https://doi.org/10.1029/2007jd008646

Fridlind, A. M., Van Diedenhoven, B., Ackerman, A. S., Avramov, A., Mrowiec, A., Morrison, H., & Shupe, M. D. (2012). A FIRE-ACE/SHEBA case study of mixed-phase Arctic boundary layer clouds: Entrainment rate limitations on rapid primary ice nucleation processes. *Journal of the Atmospheric Sciences*, *69*(1), 365–389. https://doi.org/10.1175/jas-d-11-052.1

Golaz, J.-C. (1997). *Development of a single-column model for simulating precipitating stratocumulus clouds*. Colorado State University.

Harrington, J. Y. (1997). *The effects of radiative and microphysical processes on simulated warm and transition season Arctic stratus*. (Doctoral dissertation). Colorado State University.

Harrington, J. Y., & Olsson, P. Q. (2001). On the potential influence of ice nuclei on surface-forced marine stratocumulus cloud dynamics. *Journal of Geophysical Research*, *106*(D21), 27473–27484. https://doi.org/10.1029/2000jd000236

Harrington, J. Y., Reisin, T., Cotton, W. R., & Kreidenweis, S. M. (1999). Cloud resolving simulations of Arctic stratus: Part II: Transition-season clouds. *Atmospheric Research*, *51*(1), 45–75. https://doi.org/10.1016/s0169-8095(98)00098-2

Harrington, J. Y., Sulia, K., & Morrison, H. (2013). A method for adaptive habit prediction in bulk microphysical models. Part I: Theoretical development. *Journal of the Atmospheric Sciences*, *70*(2), 349–364. https://doi.org/10.1175/jas-d-12-040.1

Henderson, G. R., Barrett, B. S., Wachowicz, L. J., Mattingly, K. S., Preece, J. R., & Mote, T. L. (2021). Local and remote atmospheric circulation drivers of Arctic change: A review. *Frontiers in Earth Science*, *9*, 709896. https://doi.org/10.3389/feart.2021.709896

Hoffmann, F. (2020). Effects of entrainment and mixing on the Wegener–Bergeron–Findeisen process. *Journal of the Atmospheric Sciences*, *77*(6), 2279–2296. https://doi.org/10.1175/jas-d-19-0289.1

Intrieri, J. M., Fairall, C. W., Shupe, M. D., Persson, P. O. G., Andreas, E. L., Guest, P. S., & Moritz, R. E. (2002). An annual cycle of Arctic surface cloud forcing at SHEBA. *Journal of Geophysical Research*, *107*(C10), SHE13-1–SHE13-14. https://doi.org/10.1029/2000jc000439

Jensen, A. A., Harrington, J. Y., Morrison, H., & Milbrandt, J. A. (2017). Predicting ice shape evolution in a bulk microphysics model. *Journal of the Atmospheric Sciences*, *74*(6), 2081–2104. https://doi.org/10.1175/jas-d-16-0350.1

Korolev, A., & Isaac, G. (2003). Phase transformation of mixed-phase clouds. *Quarterly Journal of the Royal Meteorological Society: A Journal of the Atmospheric Sciences, Applied Meteorology and Physical Oceanography*, *129*(587), 19–38. https://doi.org/10.1256/qj.01.203

McFarquhar, G. M., Ghan, S., Verlinde, J., Korolev, A., Strapp, J. W., Schmid, B., et al. (2011). Indirect and semi-direct aerosol campaign: The impact of Arctic aerosols on clouds. *Bulletin of the American Meteorological Society*, *92*(2), 183–201. https://doi.org/10.1175/2010bams2935.1

Meyers, M. P., DeMott, P. J., & Cotton, W. R. (1992). New primary ice-nucleation parameterizations in an explicit cloud model. *Journal of Applied Meteorology and Climatology*, *31*(7), 708–721. https://doi.org/10.1175/1520-0450(1992)031<0708:npinpi>2.0.co;2

Moeng, C. H., Cotton, W. R., Bretherton, C., Chlond, A., Khairoutdinov, M., Krueger, S., et al. (1996). Simulation of a stratocumulus-topped planetary boundary layer: Intercomparison among different numerical codes. *Bulletin of the American Meteorological Society*, *77*(2), 261–278. https://doi.org/10.1175/1520-0477(1996)077<0261:soastp>2.0.co;2

Morrison, H., de Boer, G., Feingold, G., Harrington, J., Shupe, M. D., & Sulia, K. (2012). Resilience of persistent Arctic mixed-phase clouds. *Nature Geoscience*, *5*(1), 11–17. https://doi.org/10.1038/ngeo1332

Morrison, H., Thompson, G., & Tatarskii, V. (2009). Impact of cloud microphysics on the development of trailing stratiform precipitation in a simulated squall line: Comparison of one-and two-moment schemes. *Monthly Weather Review*, *137*(3), 991–1007. https://doi.org/10.1175/2008mwr2556.1

Murray, B. J., O'Sullivan, D., Atkinson, J. D., & Webb, M. E. (2012). Ice nucleation by particles immersed in supercooled cloud droplets. *Chemical Society Reviews*, *41*(19), 6519–6554. https://doi.org/10.1039/c2cs35200a

Neggers, R. A. J., Ackerman, A. S., Angevine, W. M., Bazile, E., Beau, I., Blossey, P. N., et al. (2017). Single-column model simulations of subtropical marine boundary-layer cloud transitions under weakening inversions. *Journal of Advances in Modeling Earth Systems*, *9*(6), 2385–2412. https://doi.org/10.1002/2017ms001064

Neggers, R. A. J., Chylik, J., Egerer, U., Griesche, H., Schemann, V., Seifert, P., & Macke, A. (2019). Local and remote controls on arctic mixed-layer evolution. *Journal of Advances in Modeling Earth Systems*, *11*(7), 2214–2237. https://doi.org/10.1029/2019ms001671

Ovchinnikov, M., Ackerman, A. S., Avramov, A., Cheng, A., Fan, J., Fridlind, A. M., et al. (2014). Intercomparison of large-eddy simulations of Arctic mixed-phase clouds: Importance of ice size distribution assumptions. *Journal of Advances in Modeling Earth Systems*, *6*(1), 223–248. https://doi.org/10.1002/2013ms000282

Ovchinnikov, M., Korolev, A., & Fan, J. (2011). Effects of ice number concentration on dynamics of a shallow mixed-phase stratiform cloud. *Journal of Geophysical Research*, *116*(D1), D00T06. https://doi.org/10.1029/2011JD015888

Persson, P. O. G., Fairall, C. W., Andreas, E. L., Guest, P. S., & Perovich, D. K. (2002). Measurements near the Atmospheric surface flux group tower at SHEBA: Near-surface conditions and surface energy budget. *Journal of Geophysical Research*, *107*(C10), SHE–21. https://doi.org/10.1029/2000jc000705

Persson, P. O. G., Shupe, M. D., Perovich, D., & Solomon, A. (2017). Linking atmospheric synoptic transport, cloud phase, surface energy fluxes, and sea-ice growth: Observations of midwinter SHEBA conditions. *Climate Dynamics*, *49*(4), 1341–1364. https://doi.org/10.1007/s00382-016-3383-1

Pinto, J. O. (1998). Autumnal mixed-phase cloudy boundary layers in the Arctic. *Journal of the Atmospheric Sciences*, *55*(11), 2016–2038. https://doi.org/10.1175/1520-0469(1998)055<2016:ampcbl>2.0.co;2

Prenni, A. J., Harrington, J. Y., Tjernström, M., DeMott, P. J., Avramov, A., Long, C. N., et al. (2007). Can ice-nucleating aerosols affect Arctic seasonal climate? *Bulletin of the American Meteorological Society*, *88*(4), 541–550. https://doi.org/10.1175/bams-88-4-541

Rauterkus, R., & Ansorge, C. (2020). Cloud-top entrainment in mixed-phase stratocumulus and its process-level representation in large-eddy simulation. *Journal of the Atmospheric Sciences*, *77*(12), 4109–4127. https://doi.org/10.1175/jas-d-19-0221.1

Schubert, W. H., Wakefield, J. S., Steiner, E. J., & Cox, S. K. (1979). Marine stratocumulus convection. Part II: Horizontally inhomogeneous solutions. *Journal of the Atmospheric Sciences*, *36*(7), 1308–1324. https://doi.org/10.1175/1520-0469(1979)036<1308:mscpih>2.0.co;2

Shupe, M. D., & Intrieri, J. M. (2004). Cloud radiative forcing of the Arctic surface: The influence of cloud properties, surface albedo, and solar zenith angle. *Journal of Climate*, *17*(3), 616–628. https://doi.org/10.1175/1520-0442(2004)017<0616:crfota>2.0.co;2

Shupe, M. D., Persson, P. O. G., Brooks, I. M., Tjernström, M., Sedlar, J., Mauritsen, T., et al. (2013). Cloud and boundary layer interactions over the Arctic sea ice in late summer. *Atmospheric Chemistry and Physics*, *13*(18), 9379–9399. https://doi.org/10.5194/acp-13-9379-2013

Silber, I., McGlynn, P. S., Harrington, J. Y., & Verlinde, J. (2021). Habit-dependent vapor growth modulates Arctic supercooled water occurrence. *Geophysical Research Letters*, *48*(10), e2021GL092767. https://doi.org/10.1029/2021gl092767

Simpfendoerfer, L. F., Verlinde, J., Harrington, J. Y., Shupe, M. D., Chen, Y. S., Clothiaux, E. E., & Golaz, J. C. (2019). Formation of Arctic stratocumuli through atmospheric radiative cooling. *Journal of Geophysical Research: Atmospheres*, *124*(16), 9644–9664. https://doi.org/10.1029/2018jd030189

Solomon, A., Morrison, H., Persson, O., Shupe, M. D., & Bao, J. W. (2009). Investigation of microphysical parameterizations of snow and ice in Arctic clouds during M-PACE through model–observation comparisons. *Monthly Weather Review*, *137*(9), 3110–3128. https://doi.org/10.1175/2009mwr2688.1

Stevens, B., Moeng, C. H., Ackerman, A. S., Bretherton, C. S., Chlond, A., de Roode, S., et al. (2005). Evaluation of large-eddy simulations via observations of nocturnal marine stratocumulus. *Monthly Weather Review*, *133*(6), 1443–1462. https://doi.org/10.1175/mwr2930.1

Stramler, K., Del Genio, A. D., & Rossow, W. B. (2011). Synoptically driven Arctic winter states. *Journal of Climate*, *24*(6), 1747–1762. https://doi.org/10.1175/2010jcli3817.1

Sulia, K. J., & Harrington, J. Y. (2011). Ice aspect ratio influences on mixed-phase clouds: Impacts on phase partitioning in parcel models. *Journal of Geophysical Research*, *116*(D21), D21309. https://doi.org/10.1029/2011jd016298

Sulia, K. J., Morrison, H., & Harrington, J. Y. (2014). Dynamical and microphysical evolution during mixed-phase cloud glaciation simulated using the bulk adaptive habit prediction model. *Journal of the Atmospheric Sciences*, *71*(11), 4158–4180. https://doi.org/10.1175/jas-d-14-0070.1

Tan, I., & Barahona, D. (2022). The impacts of immersion ice nucleation parameterizations on Arctic mixed-phase stratiform cloud properties and the Arctic radiation budget in GEOS-5. *Journal of Climate*, *35*(13), 4049–4070. https://doi.org/10.1175/jcli-d-21-0368.1

Turner, D. D., Vogelmann, A. M., Austin, R. T., Barnard, J. C., Cady-Pereira, K., Chiu, J. C., et al. (2007). Thin liquid water clouds: Their importance and our challenges. *Bulletin of the American Meteorological Society*, *88*(2), 177–190. https://doi.org/10.1175/bams-88-2-177

van der Dussen, J. J., de Roode, S. R., & Siebesma, A. P. (2016). How large-scale subsidence affects stratocumulus transitions. *Atmospheric Chemistry and Physics*, *16*(2), 691–701. https://doi.org/10.5194/acp-16-691-2016

Verlinde, J., Harrington, J. Y., McFarquhar, G. M., Yannuzzi, V. T., Avramov, A., Greenberg, S., et al. (2007). The mixed-phase Arctic cloud experiment. *Bulletin of the American Meteorological Society*, *88*(2), 205–222. https://doi.org/10.1175/bams-88-2-205

Walko, R. L., Cotton, W. R., Meyers, M. P., & Harrington, J. Y. (1995). New RAMS cloud microphysics parameterization part I: The single-moment scheme. *Atmospheric Research*, *38*(1–4), 29–62. https://doi.org/10.1016/0169-8095(94)00087-t

Young, G., Connolly, P. J., Dearden, C., & Choularton, T. W. (2018). Relating large-scale subsidence to convection development in Arctic mixed-phase marine stratocumulus. *Atmospheric Chemistry and Physics*, *18*(3), 1475–1494. https://doi.org/10.5194/acp-18-1475-2018

Zhang, M., Xie, S., Liu, X., Lin, W., Zhang, K., Ma, H. Y., & Zhang, Y. (2020). Toward understanding the simulated phase partitioning of Arctic single-layer mixed-phase clouds in E3SM. *Earth and Space Science*, *7*(7), e2020EA001125. https://doi.org/10.1029/2020ea001125